THE OFFICIAL MAGAZINE OF THE OCEANOGRAPHY SOCIETY

Oceanography

CITATION

Thomson, J., and J. Girton. 2017. Sustained measurements of Southern Ocean air-sea coupling from a Wave Glider autonomous surface vehicle. *Oceanography* 30(2):104–109, https://doi.org/10.5670/oceanog.2017.228.

DOI

https://doi.org/10.5670/oceanog.2017.228

Sustained Measurements of Southern Ocean Air-Sea Coupling from a Wave Glider Autonomous Surface Vehicle

By Jim Thomson and James Girton

ABSTRACT. The four-month mission of a Wave Glider in the Southern Ocean has demonstrated the capability for an autonomous surface vehicle to make sustained measurements of air-sea interactions in remote regions. Several new sensor payloads were integrated for this mission, including a three-axis sonic anemometer for turbulent wind stress estimation and a high-resolution atmospheric pressure gage. The mission focused on Drake Passage, where strong gradients are common along the Antarctic Circumpolar Current (ACC) fronts. Using satellite data products, pilots ashore were able to remotely navigate the Wave Glider across the ACC Polar Front and measure changes in air-sea coupling. The resulting data set combines the persistence of a mooring with the adaptability of a ship-based survey.

INTRODUCTION

The Southern Ocean is a dynamic environment, constantly forced by winds and waves at the surface. The Antarctic Circumpolar Current (ACC) is a central feature of this region, transporting climate-relevant quantities such as ocean heat and carbon through the Antarctic system. The global connections are strong; the ACC provides a source for the overturning circulation of all three ocean basins, with important implications for future modifications of the climate system with changing surface temperatures and wind speeds (Marshall and Speer, 2012). Already, recent observations and model predictions suggest that increasing winds may be modifying the ACC and the Southern Ocean's carbon uptake (Le Quéré et al., 2007; Boning et al., 2008; Swart and Fyfe, 2012; Weller, 2015).

In Drake Passage, the ACC is squeezed laterally by Cape Horn and the Antarctic Peninsula and vertically by seafloor topography. Here, the ACC fractures into a mess of swirling eddies and meanders in the mean path. The region is characterized by strong fronts and sharp gradients, where air-ocean coupling can change significantly over a few kilometers.

Historically, the Southern Ocean is dramatically undersampled. This is changing, with long-term mooring deployments and the US National Science Foundation's Ocean Observing Initiative. However, these moorings are far from Drake Passage and its strong eddies. The only sustained measurements in Drake Passage have been regular surveys of opportunity by ARSV *Laurence M. Gould* as it crosses the passage to supply and support Palmer Station (Rintoul et al, 2010; National Research Council, 2011; Bourassa et al., 2013) and Argo profiling floats drifting through the region. The *Gould* surveys occur approximately two days out of every three weeks, so the temporal coverage is less than 10%.

A successful mission with a Wave Glider autonomous surface vehicle (ASV) was completed in Drake Passage during austral summer of 2017, expanding our ability to observe and understand this gateway of the Antarctic Circumpolar Current and the Southern Ocean. The ASV was operated both in a survey mode and in a station-keeping mode, mimicking the more traditional shipboard- and mooring-based approaches, respectively. The collected data are unique in their combination of temporal persistence and spatial coverage. Data analysis is underway and will focus on the sharp spatial gradients and strong fronts common to the region. We seek to understand air-sea coupling processes and to quantify the skill of numerical models in representing these processes.

MISSION OBJECTIVES

The goals of the Wave Glider mission were to demonstrate effective autonomous surface operations in the Southern Ocean, to study air processes in Drake Passage, and to evaluate the fidelity of model products in the region. Quantifying and working across spatial gradients was a particular focus, as these are often undersampled by traditional methods and under-resolved by numerical models.

THE AUTONOMOUS APPROACH

We instrumented a Wave Glider SV3 ASV for sustained meteorological and oceanographic measurements in Drake Passage. The Wave Glider harnesses wave motion

for propulsion using a subsurface body with passively pitching wings. The wings cause the sub to move forward with the passage of each wave, but not backward. The sub tows a surface float that contains computers for navigation and management of scientific sensors. A battery bank on the surface float powers the computers and instrumentation, and this bank is charged daily via solar panels. Autonomous navigation uses waypoints and routes established (or changed) via Iridium satellite messages. Autonomous navigation includes vessel avoidance, wherein the Wave Glider moves away from the track line of any vessels broadcasting on the Automated Information System.

The recent successes of Lenain and Melville (2014), Farrar et al. (2015), Fitzpatrick et al. (2015), and Mitarai and McWilliams (2016) demonstrate that the Wave Glider can operate and collect data continuously under full ocean conditions, even in tropical cyclones. Our Wave Glider, SV3-153, included the standard met-ocean (METOC) package offered by Liquid Robotics Inc., as used in these previous studies. The METOC package has:

- A weather station (Airmar WX200) on the float
- A Sea-Bird CTD on the sub
- An acoustic Doppler current profiler (ADCP, RDI 300 kHz) on the float
- A wave sensor (Datawell) on the float
- A GPS-based wave senor (Microstrain) on the float

In addition, we integrated several new sensors, with the goal of improving measurements of air-ocean coupling. The newly integrated sensors are:

- A three-axis ultrasonic anemometer (Gill Windmaster) on the float
- A conductivity-temperature (CT, Aanderaa) probe on the float
- A temperature-pressure-humidity probe (Paroscientific MET4) on the float

These sensors are fully integrated, with onboard data processing and telemetry as part of the existing Wave Glider payload packets and delivery/display in the web-based Wave Glider Management System (WGMS).

Figure 1 shows the Wave Glider and sensors. These sensors were evaluated during a one-week test mission on the Washington coast in July 2016, prior to the Southern Ocean deployment in December 2016. Significant concerns with each sensor are the potential for wave-motion contamination and biases associated with mounting so close to the water surface. These contaminations are removed, to first order, in post-processing. In some cases, only a subset of the data is usable. For example, the three-axis ultrasonic anemometer can only be used to estimate turbulent wind stress when the vehicle is headed into the wind (and thus the Gill Windmaster is not measuring in the wake of the other masts or antennae).

The Wave Glider was deployed on December 12, 2016, from ARSV *Laurence M. Gould* on the continental shelf of the Antarctic Peninsula, near Palmer Station. The vehicle spent a few weeks surveying across the shelf, then headed out into Drake Passage. The full track is shown in Figure 2, overlaid on the sea surface temperature field given by the MUR (Multi-scale Ultra-high Resolution; https://mur.jpl.nasa.gov) product. The zig-zag pattern in the middle of Drake Passage was designed to survey the strong fronts and meanders of the ACC common to that region. Much of this survey was done adaptively and in near-real time. Pilots ashore used AVISO (https://www.aviso.altimetry.fr) multi-satellite sea surface height maps to locate features of interest and then sent the Wave Glider a series of waypoints to sample the features. These waypoints were updated several times as AVISO maps changed.

Toward the end of the mission, solar charging was insufficient to maintain the batteries, and thus scientific payloads were disabled. No data were collected

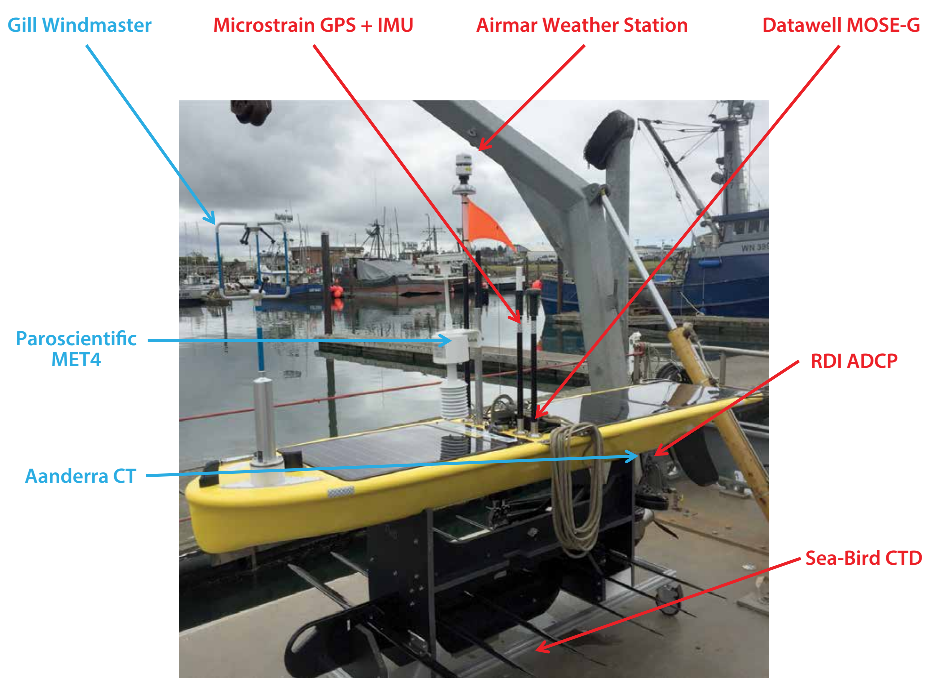

FIGURE 1. Wave Glider SV3 and instrumentation. Red labels are standard on the met-ocean version of the SV3. Blue labels are additional instrumentation integrated for this mission.

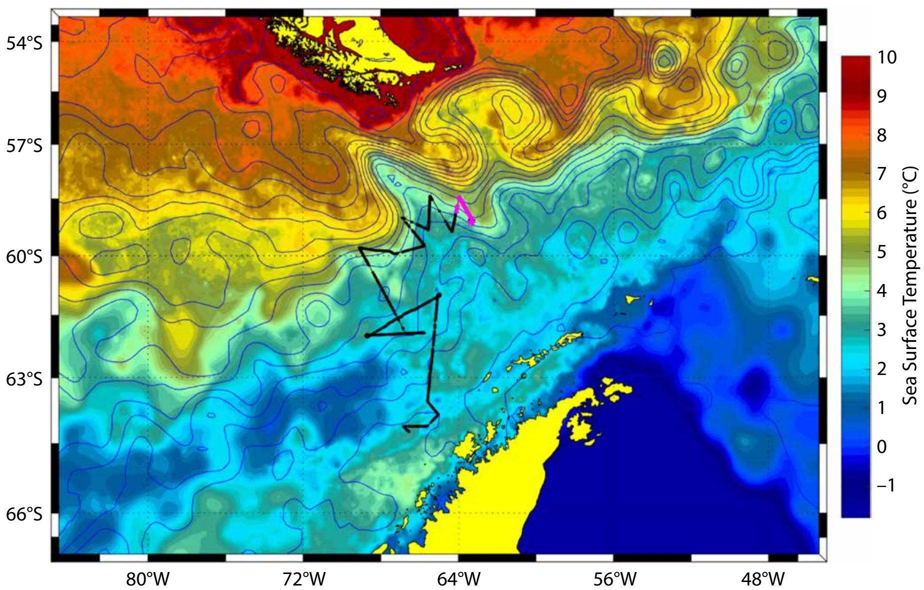

FIGURE 2. Wave Glider track while surveying Drake Passage drawn on a sea surface temperature (°C) image from the MUR (Multi-scale Ultra-high Resolution) product from January 21, 2017. The magenta portion at the end of the track, which shows five days of glider operation prior to the image date, is the focus region in an example front crossing. Solid contours indicate AVISO sea surface height (10 cm contour interval), also from January 21, 2017.

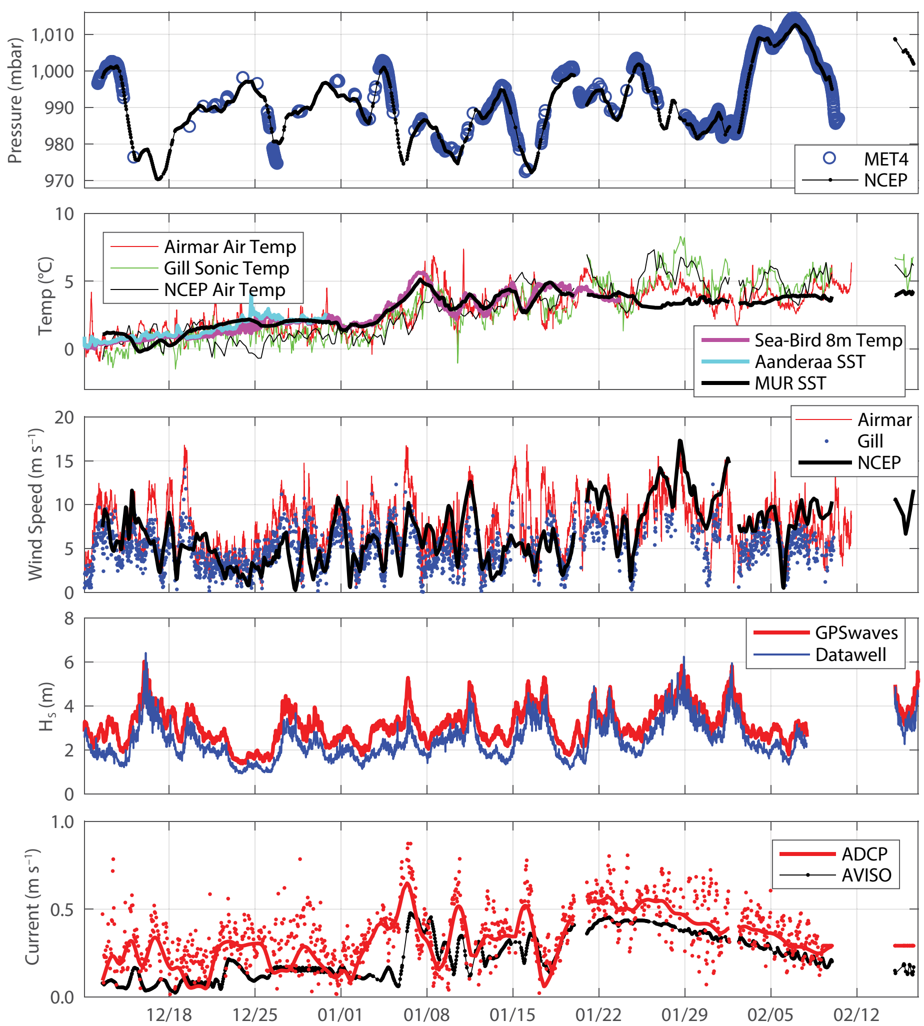

from late February until March 26, 2017, when the Wave Glider was recovered by *Gould*. This shortage of power is a severe limitation for working at high latitudes in late summer. SV3-153 was equipped with two additional auxiliary power units in anticipation of this challenge, and yet data collection still ended prematurely. Future missions will need to be more conservative in mission planning and power management.

DATA QUALITY AND NCEP MODEL COMPARISON

Figure 3 shows a full time series of the observed bulk air-sea observations, along with time series from National Centers for Environmental Prediction (NCEP) reanalysis products (Saha, 2010) and gridded data sets that have been matched to Wave Glider locations. The values are 30-minute averages or statistical estimates (e.g., significant wave height). There is generally good agreement between the bulk observations and the NCEP products, with some notable differences. Atmospheric pressure (top panel) agrees well compared to the newly integrated Paroscientific MET4 sensor, but not the standard Airmar sensor (not shown). The Airmar atmospheric pressure record is degraded onboard the instrument by referencing to instantaneous GPS elevation, which renders the signal quite noisy.

Wind speeds from both the newly integrated Gill Windmaster and the standard Airmar agree well, albeit with systematic biases (as expected from low mounting heights); observed winds are at 0.6 m and 0.9 m heights, respectively. For subsequent analyses, these wind measurements are adjusted to a standard 10 m reference height.

FIGURE 3. Full time series of major parameters collected onboard the Wave Glider. For each panel, a black line shows the gridded product (MUR, AVISO, or NCEP reanalysis) as a reference. As in Figure 1 (except in the fourth panel), red or magenta colors are Liquid Robotics Inc. standard instruments, and blue or green colors are newly integrated sensors specific to this mission.

Wave heights agree well between the two sensors, with bias high in the custom GPS sensor relative to the Datawell reference. During the 2017 Drake Passage work, we found the relative bias to be approximately 5% and appears to be most prominent at low frequencies (e.g., low-amplitude swells).

Ocean currents agree well on long time scales. On shorter time scales, the observed currents include both real high-frequency signals (inertial, tidal) and spurious heading-dependent errors. Quality control of these high-frequency data will be intensive, as the signals are not entirely independent; in some cases, vehicle navigation (and thus heading) was constrained by the strong near-inertial currents.

Future work using these observations will focus on estimating fluxes of momentum and heat by post-processing the raw data for direct covariance fluxes. These will be compared with bulk formulae and reanalysis products.

EXAMPLE OF AIR-OCEAN COUPLING ACROSS A FRONT

One process we will investigate in upcoming data analysis is the air-ocean coupling occurring across the gradients of the ACC front. The second half of the mission included several crossings of the Polar Front, one of the two strongest ACC fronts in Drake Passage (Figure 2). Figure 4 shows these crossings in detail, including the ocean currents and the water temperatures. There are strong changes in the water temperature crossing these fronts, and these are mirrored in the air temperature patterns. At large scales, the products capture these gradients. At small scales, the fidelity is much lower.

Figure 5 shows the overall correlation of air and water temperatures, which is significant at the 95% level. Absent other forcing, the air and the ocean exchange heat based on the difference in their temperatures, working toward equilibrium. This is complicated by differential transport of the air and the water, as often occurs with the strong winds common to the Southern Ocean. Sustained sampling with the Wave Glider enables multiple crossings of the front so that we can observe this spatial signal as it evolves in time (with changing forcing). With higher winds, more variability in air-ocean temperature coupling is expected, and the air-ocean temperature fronts may in turn affect the local wind forcing (Small et al., 2008; O'Neill et al., 2012).

WIND AND WAVE COUPLING

Another example of the air-ocean coupling we will investigate in upcoming data analysis is the time-space evolution of surface waves, which are forced by the almost continual winds over the Southern Ocean. By making sustained measurements, we sampled a large range of wind speeds and wave heights (see histograms in Figure 6a). The wave conditions

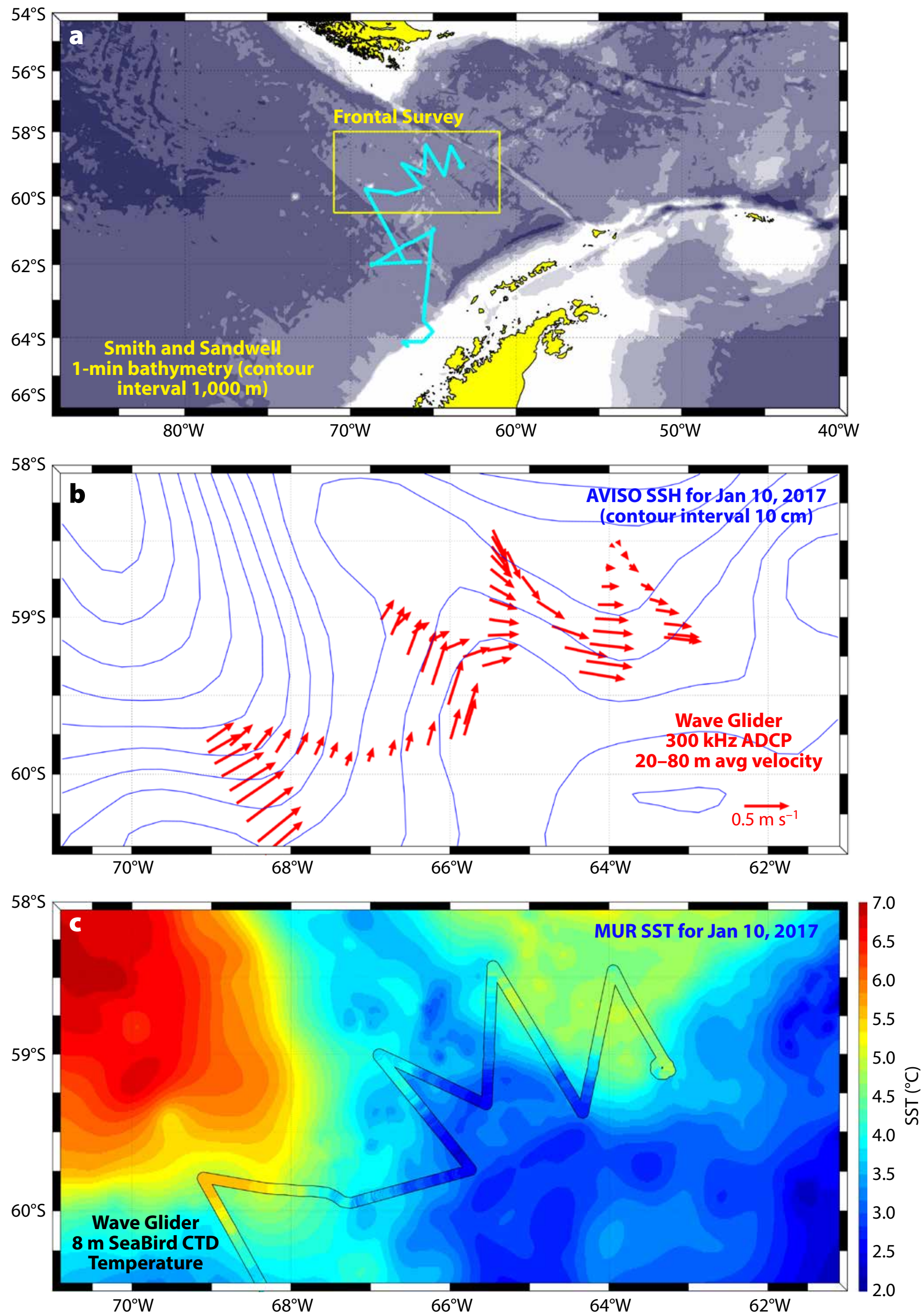

FIGURE 4. Drake Passage bathymetry, with inset showing the region surrounding the Wave Glider track from January 6–19, 2017, while crossing the Polar Front of the Antarctic Circumpolar Current (a), with ocean currents (b), and with sea surface temperature (c). This figure shows some of the same eddy fields as in Figure 2, but for January 10, 2017.

can be sorted into swell, composed of mature waves no longer forced directly by the local wind, and sea, waves forced directly by the local winds. The separation of these conditions uses the concept of wave field that is fully developed at a given local wind speed (Pierson and Moskowitz, 1964); if the waves exceed the fully developed limit, they must have a strong nonlocal source, and are therefore termed swell. Our sustained measurements cover the continuum between these distinctions.

Although the swell waves are no longer directly forced by the winds, the shorter waves in any conditions are still coupled to the winds. This is evident in the correlation of wave steepness and wind speed across all conditions, as shown in Figure 6b. This analysis uses the wave steepness from the integrated fourth moment of the wave energy spectrum (e.g., Schwendeman and Thomson, 2015). Although the high-frequency portion of the spectrum dominates this steepness metric, it does describe all the wave scales.

Thus, a mixed condition of swell and sea is a more accurate description of the Southern Ocean. Our upcoming data analysis will explore wind-wave evolution and the subsequent wave influences on the air-ocean exchange of heat and momentum. Inclusion of wave effects in air-ocean exchange is an active area of research; there are several recent parameterizations that can be tested (e.g., Oost et al., 2002; Foreman and Emeis, 2012; Garcia-Nava et al., 2012; Takagaki et al., 2012).

These wave analyses will tie back to questions of ocean transport and mixing. For example, it has been suggested that the wave-driven Stokes drift carries a significant fraction of the upper ocean momentum in the Southern Ocean (McWilliams and Restrepo, 1999) and is an integral part of the wind-driven Ekman spiral.

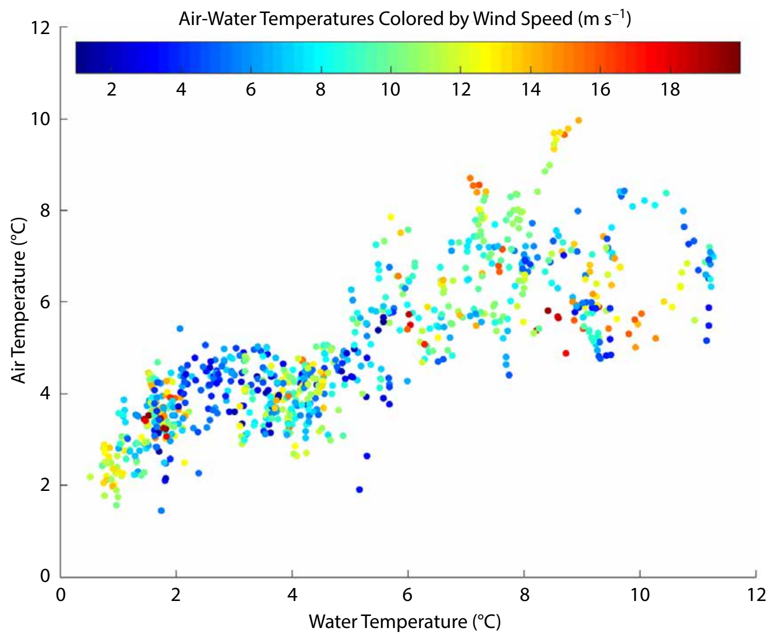

FIGURE 5. Correlation of air and water temperatures, colored by wind speeds, during the front crossing survey.

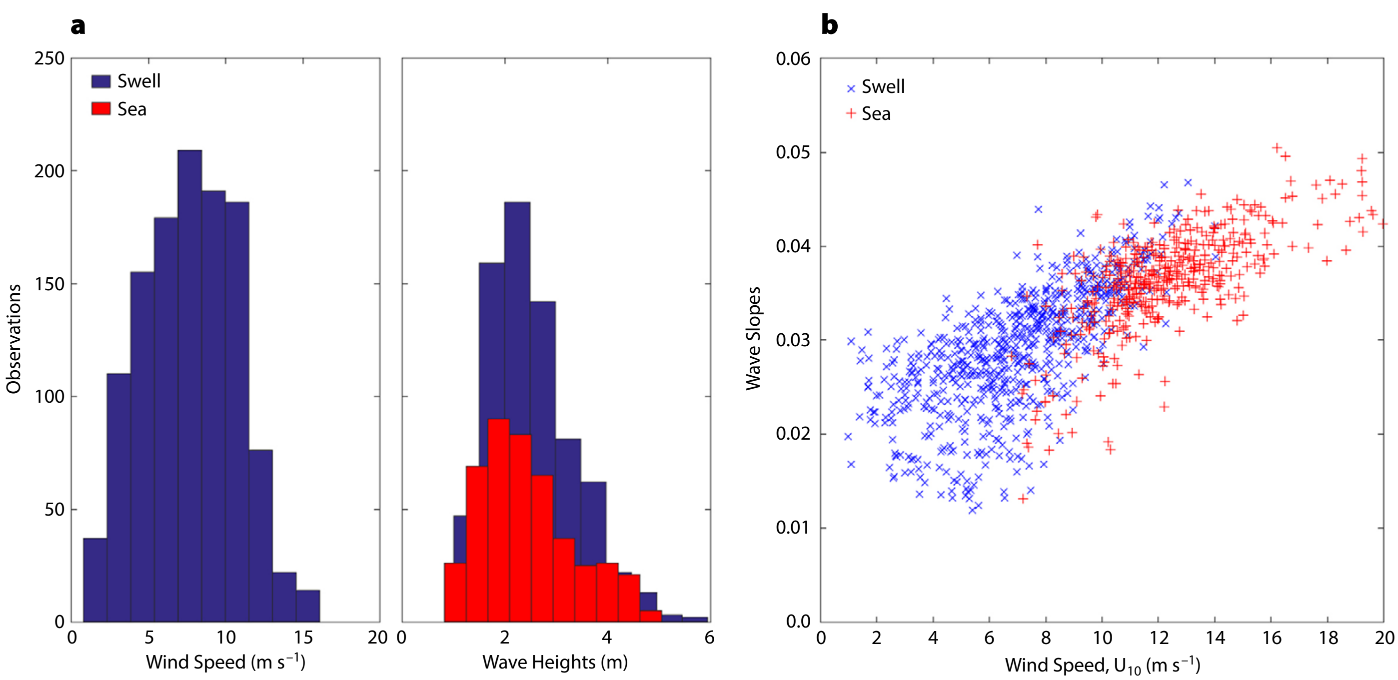

FIGURE 6. (a) Wind and wave histograms, with separation by sea (red) and swell (blue). (b) Wave slopes versus wind speeds, with separation of sea and swell.

REFERENCES

Boning, C.W., A. Dispert, M. Visbeck, S. Rintoul, and F.U. Schwarzkopf. 2008. The response of the Antarctic Circumpolar Current to recent climate change. *Nature Geoscience* 1:864–869, https://doi.org/10.1038/ngeo362.

Bourassa, M.A., S.T. Gille, C. Bitz, D. Carlson, I. Cerovecki, C.A. Clayson, M.F. Cronin, W.M. Drennan, C.W. Fairall, R.N. Hoffman, and others. 2013. High-latitude ocean and sea ice surface fluxes: Challenges for climate research. *Bulletin of the American Meteorological Society* 94:403–423, https://doi.org/10.1175/BAMS-D-11-00244.1.

Farrar, J.T., L. Rainville, A.J. Plueddemann, W.S. Kessler, C. Lee, B.A. Hodges, R.W. Schmitt, J.B. Edson, S.C. Riser, C.C. Eriksen, and D.M. Fratantoni. 2015. Salinity and temperature balances at the SPURS central mooring during fall and winter. *Oceanography* 28(1):56–65, https://doi.org/10.5670/oceanog.2015.06.

Fitzpatrick, P.J., Y. Lee, R. Moorhead, A. Skarke, D. Merritt, K. Kreider, C. Brown, R. Carlon, G. Hine. T. Lampoudi, and A.P. Leonardi. 2015. A review of the 2014 Gulf of Mexico Wave Glider field program. *Marine Technology Society Journal* 49:64–71, https://doi.org/10.4031/MTSJ.49.3.14.

Foreman, R., and S. Emeis. 2012. Correlation equation for the marine drag coefficient and wave steepness. *Ocean Dynamics* 62:1,323–1,333, https://doi.org/10.1007/s10236-012-0565-1.

Garcia-Nava, H., F.J. Ocampo-Torres, P.A. Hwang, and P. Osuna. 2012. Reduction of wind stress due to swell at high wind conditions. *Journal of Geophysical Research* 117, C00J11, https://doi.org/10.1029/2011JC007833.

Lenain, L., and W.K. Melville. 2014. Autonomous surface vehicle measurements of the ocean's response to Tropical Cyclone Freda. *Journal of Atmospheric and Oceanic Technology* 31(10):2,169–2,190, https://doi.org/10.1175/JTECH-D-14-00012.1.

Le Quéré, C., C. Rödenbeck, E.T. Buitenhuis, T.J. Conway, R. Langenfelds, and A. Gom. 2007. Saturation of the Southern Ocean CO_2 sink due to recent climate change. *Science* 316:1,735–1,738, https://doi.org/10.1126/science.1136188.

Marshall, J., and K. Speer. 2012. Closure of the meridional overturning circulation through Southern Ocean upwelling. *Nature Geoscience* 5:171–180, https://doi.org/10.1038/ngeo1391.

McWilliams, J.C., and J.M. Restrepo. 1999. The wave-driven ocean circulation. *Journal of Physical Oceanography* 29:2,523–2,540, https://doi.org/10.1175/1520-0485(1999)029<2523:TWDOC>2.0.CO;2.

Mitarai, S., and J.C. McWilliams. 2016. Wave Glider observations of surface winds and currents in the core of Typhoon Danas. *Geophysical Research Letters* 43:11,312–11,319, https://doi.org/10.1002/2016GL071115.

National Research Council. 2011. *Future Science Opportunities in Antarctica and the Southern Ocean*. The National Academies Press, Washington, DC, https://doi.org/10.17226/13169.

O'Neill, L.W., D.B. Chelton, and S.K. Esbensen. 2012. Covariability of surface wind and stress responses to sea surface temperature fronts. *Journal of Climate* 25, https://doi.org/10.1175/JCLI-D-11-00230.1.

Oost, W., G. Komen, C. Jacobs, and C. Van Oort. 2002. New evidence for a relation between wind stress and wave age from measurements during ASGAMAGE. *Boundary Layer Meteorology* 103:409–438, https://doi.org/10.1023/A:1014913624535.

Pierson, W.J. Jr., and L. Moskowitz. 1964. A proposed spectral form for fully developed wind seas based on the similarity theory of S.A. Kitaigorodskii. *Journal of Geophysical Research* 69:5,181–5,190, https://doi.org/10.1029/JZ069i024p05181.

Rintoul, S.R., K. Speer, M. Sparrow, M. Meredith, E. Hofmann, E. Fahrbach, C. Summerhayes, A. Worby, M. England, R. Bellerby, and others. 2010. Southern Ocean Observing System (SOOS): Rationale and strategy for sustained observations of the Southern Ocean. In *Proceedings of OceanObs 09: Sustained Ocean Observations and Information for Society*, vol. 2. Venice, Italy, September 21–25, 2009, J. Hall, D.E. Harrison, and D. Stammer, eds, European Space Agency Publication WPP-306, https://doi.org/10.5270/OceanObs09.cwp.74.

Saha, S., S. Moorthi, H.-L. Pan, X. Wu, J. Wang, S. Nadiga, P. Tripp, R. Kistler, J. Woollen, D. Behringer, and others. 2010. The NCEP climate forecast system reanalysis. *Bulletin of the American Meteorological Society* 91(8):1,015–1,056, https://doi.org/10.1175/2010BAMS3001.1.

Schwendeman, M., and J. Thomson. 2015. Observations of whitecap coverage and the relation to wind stress, wave slope, and turbulent dissipation. *Journal of Geophysical Research* 120:8,346–8,363, https://doi.org/10.1002/2015JC011196.

Small, R.J., S.P. DeSzoeke, S.P. Xie, L. O'Neill, H. Seo, Q. Song, P. Cornillon, M. Spall, and S. Minobe. 2008. Air-sea interaction over ocean fronts and eddies. *Dynamics of Atmospheres and Oceans* 45:274–319, https://doi.org/10.1016/j.dynatmoce.2008.01.001.

Swart, N.C., and J.C. Fyfe. 2012. Ocean carbon uptake and storage influenced by wind bias in global climate models. *Nature Climate Change* 2:47–52, https://doi.org/10.1038/nclimate1289.

Takagaki, N., S. Komori, N. Suzuki, K. Iwano, T. Kuramoto, S. Shimada, R. Kurose, and K. Takahashi. 2012. Strong correlation between the drag coefficient and the shape of the wind sea spectrum over a broad range of wind speeds. *Geophysical Research Letters* 39, L23604, https://doi.org/10.1029/2012GL053988.

Weller, R.A. 2015. Variability and trends in surface meteorology and air-sea fluxes at a site off northern Chile. *Journal of Climate* 28:3,004–3,023, https://doi.org/10.1175/JCLI-D-14-00591.1.

ACKNOWLEDGMENTS

Field engineers Alex de Klerk, Avery Snyder, and Joe Talbert helped with integration and testing of Wave Glider sensors, as well as deployment, operation, and recovery. The captain, crew, and marine technicians onboard ARSV *Laurence M. Gould* provided excellent support in deployment and recovery of the Wave Glider. Funding support was provided by the National Science Foundation (OCE1558448).

AUTHORS

Jim Thomson (jthomson@apl.washington.edu) and **James Girton** (girton@apl.washington.edu) are both Principal Oceanographers, Applied Physics Lab, University of Washington, Seattle, WA, USA.

ARTICLE CITATION

Thomson, J., and J. Girton. 2017. Sustained measurements of Southern Ocean air-sea coupling from a Wave Glider autonomous surface vehicle. *Oceanography* 30(2):104–109, https://doi.org/10.5670/oceanog.2017.228.